ON THE APPLICATION OF REMOTE SENSING TIME SERIES ANALYSIS FOR LAND COVER MAPPING: SPECTRAL INDICES FOR CROPS CLASSIFICATION

C. Collu[1], F. Dessì[1], D. Simonetti[2], P. Lasio[3], P. Botti[3], M. T. Melis [1, *]

[1] Department of Chemical and Geological Sciences, University of Cagliari, Cittadella Universitaria (BloccoA)
S.S. 554 bivio per Sestu - 09042 Monserrato (CA), Italy, titimelis@unica.it
[2] Joint Research Centre, via Enrico Fermi 2749, TP250, 21027 Ispra (VA), Italy
[3] Directorate General of the Regional Agency of the Hydrographic District of Sardinia, via Mameli 88, 09123 Cagliari, Italy

Commission III, WG III/1

KEY WORDS: Sentinel, Land cover, agricultural mapping, multispectral analysis, Sardinia
ABSTRACT:

This study aims to introduce a semi-automatic classification workflow for the production of a land use/land cover (LULC) map of the island of Sardinia (Italy) following the CORINE legend schema, and a ground spatial resolution compatible with a scale of 1:25.000. The classification is based on free high-resolution satellite imagery from Sentinel-1 and Sentinel-2 collected in 2020, ancillary data derived from Sardinian Geoportal, Joint Research Centre (JRC) and OpenStreetMap. The LULC map production includes three steps: 1) pixel-based classification, realized with two different approaches, that use i) information derived from existing thematic maps eventually re-coded in case of incoherencies observed between datasets and/or satellite data products, and ii) spectral indices and parameter thresholds defined on the basis of multitemporal analysis; 2) segmentation of Sentinel-1 and 2 annual composites, and pre-labelling of segments with the pixel-based classified map, obtaining the preliminary map; 3) visual inspection procedure in order to confirm, or re-assign, classes to polygons. The accuracy of the preliminary map was tested in a sample area and on specific class of non-irrigated crops through ground truth data collected from a detailed photo-interpretation, estimating 97% of overall accuracy. The results show a great improvement from existing thematic maps in terms of detail, with the possibility of a yearly updating of the map via automatic processes. However, some limitations were found, due to the high fragmentation of Sardinian landscape and the high variety of crop types and agricultural practices, that could affect the efficiency of the classifier.

1. INTRODUCTION

Earth Observation (EO) data can significantly contribute to improving the monitoring of land cover/land use changes. In recent years, the availability of yearly land cover maps has increased, and a large number of global products adopted the approaches based on open EO data and online cloud computing platforms (De Simone et al., 2021). These existing maps are very useful at global and regional level, and are used mainly for the extraction of indicators to estimate, for instance, climate change impacts, or applying statistical analysis. Further applications include the monitoring of agricultural areas' condition to access information related to crop types, their health and water state, optimizing the management and reduce environmental impacts. Remote sensed imagery and, in particular, spectral indices, like NDVI (Normalized Difference Vegetation Index) or EVI (Enhanced Vegetation Index), are commonly used to classify crop types, quantify the biomass and extract vegetation phenology (Castillo et al., 2017; Sanobe et al., 2018). Multitemporal analysis of spectral indices is widely applied to extract information about seasonality, useful for classification of crop types (Itzerott et al., 2006; Boschetti et al., 2014; Pageot et al., 2020; Qu et al. 2020, D'Andrimont et al. 2021). Spectral indices are also adopted to classify other land cover types, among all, water bodies, wetlands and salt surfaces (Bansal et al., 2017; Wang et al., 2018, Afrasinei et al, 2017, 2018) and urban or/and other artificial areas (Faridatul & Wu, 2019; Sinha et al., 2016).

This study aims to introduce a semi-automatic classification workflow for the production of a land use/land cover (LULC) map of the Sardinia island (Fig. 1), using free satellite high resolution imagery, with a ground spatial resolution compatible with a scale of 1:25.000. The proposed approach is aiming at i) identifying and mapping agricultural lands, according to the third and fourth level of the land cover classification proposed by the CORINE legend (https://land.copernicus.eu/user-corner/technical-library/clc product-user-manual); ii) offering the possibility of a yearly updating of the map via automatic processes, rather than by using visual interpretation. Unfortunately, due to the high Sardinian landscape fragmentation and local land use, based on small farms, existing LULC maps do not represent correctly the different land cover classes. This issue is particularly enhanced in the identification of agricultural lands. This information is often available from national database populated by the farmers or by the regional agencies, but normally they are not updated and these data are not spatially mapped. In our study, the identification of the different agriculture crops has been requested mainly to monitor the irrigation practices to optimize the water use.

2. STUDY AREA

Sardinia island is an Italian region with an extension of 24,090 km2, the second in size after Sicily among the islands of the western Mediterranean Sea (Figure 1). The coastline is long about 1,850 km, it is generally rocky with irregular shapes, some deep bays, and large beaches. The inner part is mostly

* Corresponding author

mountainous. The island's highest point is Punta La Marmora, in the Gennargentu Range, at 1,834 m above sea level. The drainage is characterized by few major rivers with a continuous water flow, and interspersed with artificial lakes and dams. Several seasonal streams, originating from the mountainous areas, shape the morphological evolution, controlled on top by the geological setting. The geological history of this island is recorded in the variety of lithologies and tectonic features that outcrop: granites, basalts, sandstones, limestones as well as metamorphic rocks as schists. Consequently, landforms and landscapes are very heterogeneous with abrupt morphologies alternating with gentle slopes. The alluvial plains are distributed along the coast, at the river mouths, where the urban areas are concentrated. Moreover, the Campidano wide plain consists of the main intensive cultivated area. With a population of about 1,640,000, Sardinia is one of the regions with the lowest population density in Italy.

Due to variations in both latitude and elevation and the presence of the sea, the climate of the island is not constant everywhere. In line with the Mediterranean climate, Sardinia receives the most part of annual rainfall during winter and fall; summer is often dry with almost no rain during June and July, and exceptional brief and heavy precipitations at the end of the summer with high impacts on the hydrogeological hazard. The temperature can rise up to 40 °C in summer.

Figure 1. Location of the study area

2.1 Land Cover in Sardinia

The first land cover map in Sardinia was realised in 1990 in the framework of European CORINE Land Cover Project (https://land.copernicus.eu/pan-european/corine-land-cover). This map was produced in Sardinia, according to the European standards, by photointerpretation of Landsat images, and in the following years was updated, using orthophotos and partially satellite data, obtaining the last available map on 2008 at the map scale of 1:25,000. In the last years, the availability of free satellite data with a global coverage and a high temporal resolution led to development of global land cover maps. Moreover, the earth dynamics monitoring became the base for climate changes evaluations, and the human impacts on the environment marked in the LULC maps has tremendous implications. So, an automatic LULC map production is felt as a necessity. Recently, the ESA WorldCover project (Zanaga et al., 2020) distributed a LULC map derived from Sentinel imagery with a 10m resolution for 2020 based on ESA Sentinel-1 and 2 data. This map has been produced through an automatic methodology and a legend of 10 classes has been applied at global scale. In Figure 2, the extent expressed in percent of land cover classes, extracted from the WorldCover map over the study region, is shown: the dominant class (almost 50%) is the tree cover, nearly close to the sum of shrubland and grassland. Built-up class is very small while cropland covers 10% of the island surface.

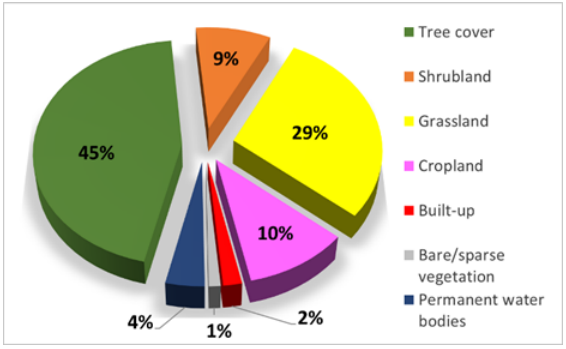

Figure 2. WorldCover map of Sardinia region: the extent of each land cover classes expressed in percent

3. MATERIALS AND METHODS

In this study, a series of available databases and existing thematic maps from Sardinian Geoportal (https://www.sardegnageoportale.it), Open Street Map and Joint Research Centre (JRC) were used. Sentinel-1 and Sentinel-2 imagery were selected for spectral indices extraction and multi-temporal analysis. In addition, AGEA (Agenzia per le Erogazioni in Agricoltura, https://www.agea.gov.it/) high-resolution orthophotos (0,20 m/pixel) were utilised for visual inspection (Table 1).

Following data pre-processing, the land cover map was realised through three steps, as displayed in Figure 3: 1) pixel-based classification, 2) image segmentation and pre-labelling of segments, 3) visual inspection of the resulting map.

3.1 Pixel-based classification

Pixel-based classification of land cover types according to CORINE legend (third or fourth level), was based on existing thematic maps and satellite data products derived from Sentinel-1 and 2, that will be described in section 4.1.

The classification schema (Figure 3) involves multi-classifiers organised in a cascade system, in which the output of the previous classifier is the input of the next classifier. Each classifier is based on a) information derived from existing thematic maps, subjected to error of omission and/or commission detecting and re-coding through observed incoherence between different thematic maps and/or satellite data products, b) spectral indices and parameter thresholds defined on the basis of multitemporal analysis of the different crops, agricultural phenology and known agronomic techniques adopted in the study area.

3.2 Segmentation and pre-labelling of segments

Segmentation process involves image partition into multiple groups of pixels, called segments or objects, with similar spectral characteristics. This process was carried out on satellite data collected in 2020 (section 4.1), potentially representing different land cover classes. In particular, segmentation was performed in IMPACT Toolbox on an image composed by three band: the GREEN and NIR band (B3 and B8 respectively) of Sentinel-2 annual composite of 2020 (section 4.1.2.1), and a band derived from the computed mean value of VV and VH polarisation bands of the Sentinel-1

Table 1. Description and source of the datasets and thematic maps

Dataset/thematic map	Source	Description
Sentinel-1, VV and VH polarizations (Level-1 GRD)	Google Earth Engine	Sentinel-1 radar data from Level-1 Ground Range Detected (GRD) Interferometric Wide Swath (IW) product. Sentinel-1 operates at C-band (central frequency of 5.404 GHz) containing VH and VV polarizations, with spatial resolution of 10, 25 or 40 m/px and a revisit cycle of 12 days.
Sentinel-2 Level-2A	Google Earth Engine	Sentinel-2 satellites provide optical images with surface coverage every 10 days at the equator with one satellite, and 5 days with two satellites under cloud-free conditions, which results in 2-3 days at mid-latitudes. Sentinel-2 images have a spatial resolution of 10 to 60 m/px, and 13 spectral bands range from the Visible (VNIR) and Near Infra-Red (NIR) to the Short Wave Infra-Red (SWIR). Level-2A product consists of orthorectified Bottom of Atmosphere (BOA) reflectance data.
Water features, roads, infrastructures, built-up	Open Street Map	OpenStreetMap features available in January 2021.
Global Human Settlement Layer	Joint Research Centre (JRC)	Multi-temporal classification map of built-up presence derived from Landsat image collections (GLS1975, GLS1990, GLS2000, and ad-hoc Landsat 8 collection 2013/2014).
Copernicus CORINE Land Cover (2018)	Google Earth Engine	Corine Land Cover (CLC) dataset of Europe with the resolution of 100m/px, produced within the Copernicus Land Monitoring Service coordinated by the European Environment Agency (EEA), on the basis of satellite image classification.
Land Use Map (2008)	Sardinian Geoportal	Land use map of Sardinia, at a scale of 1:25 000. Land use features are identified with Corine Land Cover classes.
DBGT 10k (2020): - level ST01 (viability) - level ST02 (construction) - level ST04 (hydrography) - level ST06 (vegetation)	Sardinian Geoportal	Geo-Topographic database at a scale of 1:10 000 containing geographic features related to administrative boundaries, viability, construction, hydrography, orography and vegetation, derived from aero-photogrammetric restitution on the basis of the aerial photos taken in 2013, from the Regional Technical Map and from Land Use Map of 2008.
Orthophoto (2019)	AGEA	AGEA orthophoto with spatial resolution of 0,20 m/pixel, containing 4 bands (BLUE, GREEN, RED and NIR) acquired in 2019.

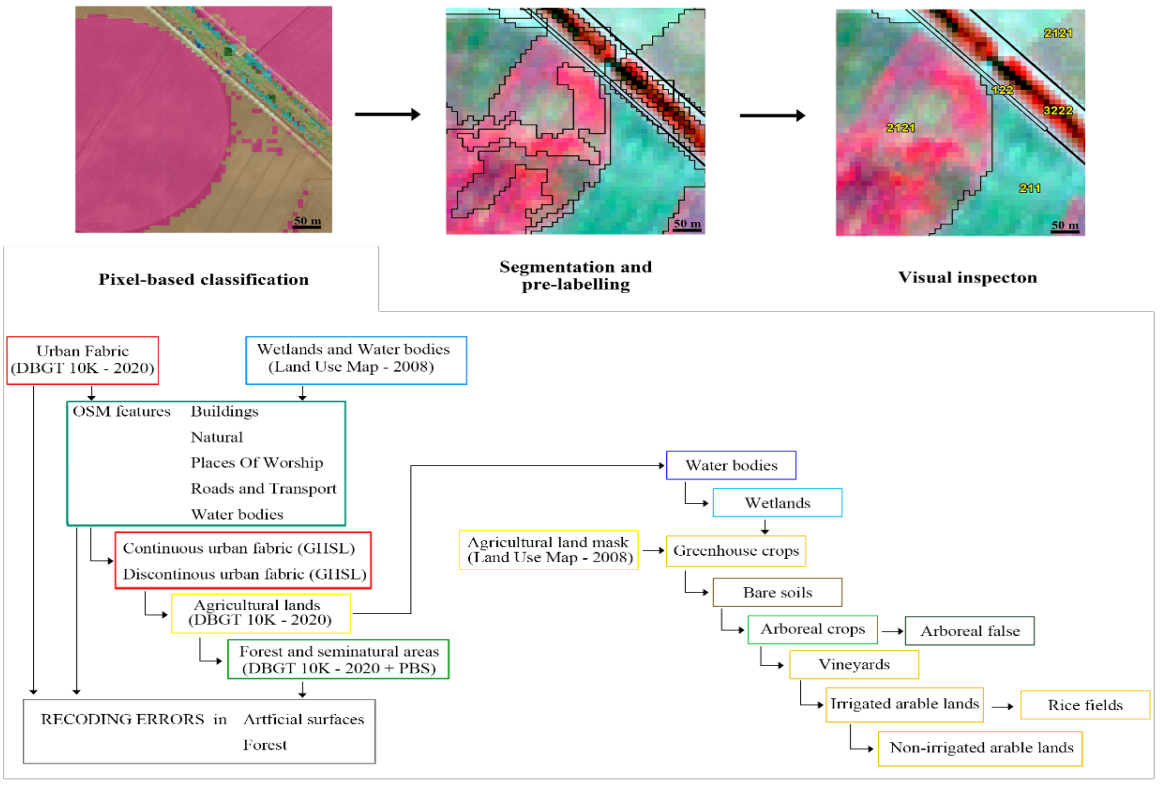

Figure 3. Workflow adopted in this study, composed by three steps: pixel-based classification, segmentation and pre-labelling and visual inspection (top), and classification schema for pixel-based classification (bottom).

annual composite of 2020 (4.1.1). The segmentation algorithm implemented in IMPACT Toolbox is based on Baatz and Schape (2000) method, with the definition of four parameters: 1) scale factor, correlated with minimum mapping unit, 2) color (0-1), Baatz spectral component, 3) compactness (0-1), Baatz morphological component, 4) similarity (0-1), related to the minimum grade of homogeneity within objects during segments merging (Joint Research Centre et al., 2015). In this study a scale factor of 4 pixels, a color of 0.9, a compactness of 0.7 and a similarity of 0.82 were used in this study.

3.3 Visual inspection

The classified product derived from segmentation has been subjected to a detailed visual inspection in a sample area in the northern part of the Campidano Plain, a sub region of Sardinia very devoted to agriculture. The visual inspection could check the goodness of the work of the classifier, proceeding with an assessment and a modification of attribute polygons in case of discrepancies. This totally manual, on-screen, control procedure confirms or re-assigns the legend codes of various polygons coming from the classification activities, also introducing spatial aggregation operations (merging) aimed to blend adjacent polygons with the same attribute. This method allows to, on the one hand, update the information extracted from existing maps and databases, and, on the other hand, detect and differentiate also the CORINE classes that cannot be extracted through automatic classifications, due to the similar spectral characteristics. The size of 1000 m^2 has been chosen as the minimum cartographic unit.

4. RESULTS AND DISCUSSION

4.1 Satellite data products

Satellite data products used for classification and segmentation, and the maps realised in this study are described and discussed below.

4.1.1 Sentinel-1

Sentinel-1 data acquired from 2019 to 2020 were selected and processed in Google Earth Engine platform using the methodology proposed by Mullissa et al. (2021), that includes speckle filtering, border noise correction and radiometric terrain normalisation. From this dataset, a biannual composite (2019-2020, annual and monthly composites of 2020 were extracted by calculating the mean value of both VV and VH polarizations. On

Sentinel-1 time series composed by the monthly composites minimum values were computed.

4.1.2 Sentinel-2

Sentinel-2 optical data acquired in a temporal window from 2017 to 2020 have been processed in Google Earth Engine platform to produce annual and monthly composites, PBS (Phenological Based Synthesis) classification and spectral indices time series.

Annual composite of 2020

From Sentinel-2 BOA (Bottom Of Reflectance) images collected during 2020, an annual composite was produced, computing the median value for each band, after cloud and relative shadows masking performed through the algorithm developed by Simonetti et al. (2021).

Monthly composites of 2020

Monthly composites of 2020 were processed by calculating, for each month, the median values of cloudless images from level-2A product, obtained with two different cloud masking methods. For summer months, characterized mainly by cloud-free images, Sentinel-2 quality assessment band (QA60) was used for the detection and masking of cloudy pixels. For the other months of the year, influenced by a higher cloud coverage, cloud masking was performed using Sentinel Hub's Cloud Probability map, that provides a probability measure in percentage of cloud or snow presence in Sentinel-2 images. Pixels with a probability higher than 30% were masked, and potential data gaps resulting from masking, were filled with the same dataset filtered with QA60 masking method. For each monthly composites, a series of spectral indices and parameters were extracted (Table 2), including NDVI (Normalised Difference Vegetation Index), NDSI (Normalised Difference Soil Index), NGRDI (Normalised Green-Red Index), Red, Green and Blue brightness. Over the NDVI time series determined from monthly composites, the median, maximum, minimum, and amplitude values were calculated, along with the time when maximum and minimum were found.

Maximum NDVI map (2017-2020)

A maximum NDVI map (Greenest pixel) was extracted over a period from 2017 to 2020, from Sentinel-2 level-2A images after the cloud masking procedure proposed by Simonetti et al. (2021).

Minimum NDVI map (2019-2020)

Reflectance data from Sentinel-2 level-2A product acquired from 2019 to 2020, and filtered through the cloud masking procedure by Simonetti et al. (2021), were processed to extract a minimum NDVI map.

Phenological Based Synthesis (PBS) Classification

The PBS classifier algorithm proposed by Simonetti et al. (2015), originally developed for Landsat imagery, has been adapted to ingest, classify and mask clouds and shadows from Sentinel-2 multispectral images using Simonetti et al. (2021). The thematic land cover classification has been obtained processing all images (295) acquired in 2019 and 2020 and provides information about vegetation and water seasonality as well as more stable classes such as bare soil or artificial built-up.

NDVI and NDFI time series

In order to investigate the seasonality of agricultural crops, multitemporal analysis was carried out on a detailed NDVI and NDFI time series, produced from a dataset composed by all BOA reflectance data (Sentinel-2 level-2A product) acquired in a temporal window between 04-01-2020 and 10-31-2020, subsequently to the same cloud masking procedure adopted for monthly composites. The resulting NDVI time series of each pixel was smoothed using a linear regression algorithm with a moving window of 22 days (Figure 4), to reduce noise derived from residual cloud cover (Boschetti et al., 2017). On the other hand, multitemporal analysis on NDFI time series was performed on the raw series, because the smoothing algorithm could mask isolated flood signals.

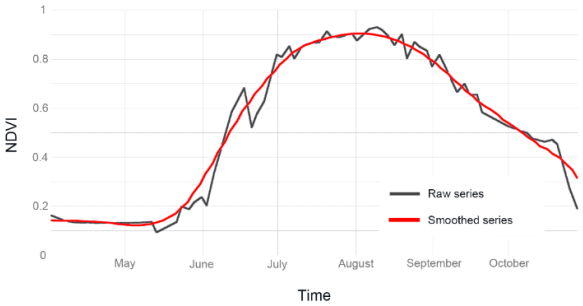

Figure 4. Raw and related smoothed curve of NDVI time series resulting from smoothing process.

Table 2. Spectral indices and parameters computed in this study

Spectral index/parameter	Formula	Description
VVmin	-	Minimum value of VV time series of Sentinel-1 monthly composites.
NDVI	$\frac{RED - NIR}{RED + NIR}$	Normalised Difference Vegetation Index, measures density and health of vegetation.
NDVImedian	-	Median value of NDVI time series of Sentinel-2 monthly composites.
NDVImax	-	Maximum value of NDVI time series of Sentinel-2 monthly composites.
NDVImin	-	Minimum value of NDVI time series of Sentinel-2 monthly composites.
Timemax	-	Time when the maximum value of NDVI was found. Timemax is expressed in month number (1-12) for the NDVI time series of monthly composites (Chapter 3.2.2), and in Day of the Year (DoY) for the detailed NDVI time series (Chapter 3.2.5).
Timemin	-	Time, expressed in month number (1-12), when the minimum value of NDVI was found.
Amplitude	NDVImax- NDVImin	Difference between maximum and minimum value of NDVI.
RB	$\frac{RED}{RED + GREEN + BLUE} * 100$	Red brightness percentage in VIS spectral range.
GB	$\frac{GREEN}{RED + GREEN + BLUE} * 100$	Green brightness percentage in VIS spectral range.
BB	$\frac{BLUE}{RED + GREEN + BLUE} * 100$	Blue brightness percentage in VIS spectral range.
NDSI	$\frac{SWIR_1 - NIR}{SWIR_1 + NIR}$	Normalised Difference Soil Index, sensitive to bare soils and artificial surfaces.
NGRDI	$\frac{GREEN - RED}{GREEN + RED}$	Normalised Green-Red Difference Index, sensitive to vegetation density.
NDFI	$\frac{RED - SWIR_1}{RED + SWIR_1}$	Normalised Difference Flood Index, sensitive to soil submergence typical of flooded rice fields (Boschetti et al., 2014).

4.2 Pixel-based classification map

Pixel-based classification of artificial surfaces, agricultural permanent crops (vineyards, olive groves and fruit trees), forest and semi-natural areas, wetlands and water bodies, was based on existing maps and databases, recoded through observed incoherence between these maps and satellite data products, and thus, represents an updated product of existing thematic maps (Figure 5). In agricultural areas, spectral indices and parameter thresholds approach was adopted in order to distinguish irrigated areas, rice fields, additional vineyards and greenhouse crops. Three more classes were integrated in the legend: arboreal crops
(fruit trees, olive groves, forest trees, etc.), false arboreal (surfaces incorrectly classified as arboreal crops) and bare soils. These crop types embrace different CORINE classes with similar spectral characteristics and thus not easily distinguishable from each other. For this reason, the correct assignment of the CORINE class for these crop types will occur through visual interpretation in the visual inspection phase. Pastures and heterogeneous agricultural areas have not been classified, as a consequence of the relevant variability that characterises these classes. The classification criteria for the agricultural lands are shown in Table 3.m. The classification on agricultural areas imported from DBGT (2020) has introduced new water bodies, wetlands and vineyards not classified in the existing maps. Moreover, the classification of arboreal crops has led to detection of new olive groves, fruit trees and forest areas classified as agricultural land in previous thematic maps. Classification issues related to water bodies, wetlands, greenhouse crops and bare soils concern mainly a confusion with new artificial surfaces (industrial or commercial units, urban, mineral extraction sites etc.) absent in previous thematic maps. Some confusion is also observed between arboreal crops, vineyards and irrigated areas that show a stable trend of NDVI during the year and a consistent photosynthetic activity in summer period, like, for example, irrigated permanent grassland, dense vegetation nearby water bodies and particularly dense vineyards. Classification of rice fields doesn't exhibit significant issues, except for some undetected rice fields, probably due to a different agricultural practice (dry-direct seeded rice, upland rice etc.).

4.3 Preliminary map

The segmentation process has generated approximately 5x106 segments over 2,4x10^4 km^2 Sardinia total area. High fragmentation is observed in urban fabric, whereas forest areas have been segmented into larger polygons, demonstrating the validity of selected segmentation parameters.
Land cover classes of the pixel-based classification were assigned to the objects resulting from segmentation process according to the majority occurrence rule, through which the assigned class is the one most frequently observed within each object.

Figure 5. An example of commission error in a coniferous plantation harvested and re-planted (white area on the right), detected as an error, considering that the area was classified as coniferous forest (dark green on the left, code 312) from existing thematic maps.

Table 3. Classification criteria for agricultural lands with the threshold of spectral indices and parameters computed in this study.

Class	Criteria or spectral indices/parameter threshold	Description
Permanent crops	Imported from DBGT 10K (2020)	As permanent crops, vineyards, olive groves and fruit trees were imported from the geo-topographic database of 2020, assuming that these types of crop remain stable for several years.
Water bodies	$NDVI_{median} < 0$	In order to detect additional water bodies and wetlands classified as agricultural areas in previous classification steps, negative values of NDVI and very low values of minimum NDVI registered over NDVI time series of monthly composites were selected. For wetlands VV_{min} was used for discrimination between water surfaces and bare soils.
Wetlands	$NDVI_{min} < 0.10$ $VV_{min} < -19$	
Greenhouse crops	$0 < NDVI_{median} < 0.35$ $NDVI_{max} < 0.55$ $NDVI_{min} < 0.15$ $VV_{min} < -18$ $\rho BLUE_{August} > 1000$ $12\ \% < (RB - BB)_{Aug} < 20\%$	Greenhouse crops are characterised by dark or very bright surfaces, with a higher reflectance in blue spectral range than natural surfaces (vegetation, soils etc.). For these reasons, low values of NDVI, minimum VV polarisation and spectral characteristics in blue and red spectral ranges were selected to detect this type of land cover.
Bare soils	$0 < NDVI_{median} < 10$	Surfaces not covered by any vegetation and not classified as water bodies, wetlands or greenhouse crops, were classified as bare soils.
Arboreal crops	$NDVI_{min} > 0.20$ Amplitude < 0.42 $\rho NIR_{August} < 3400$ $NDSI_{August} < 0.10$ $NGRDI_{August} < 0.15$	Arboreal crops include any surfaces covered by arboreal vegetation (forest, olive groves, fruit trees etc.). This type of crop is characterised by a stable trend of NDVI during the year compared to arable lands, and a NIR reflectance lower than grasslands due to the shadows produced in tree crowns (Qian et. Al, 2020). NDSI index was used for soil or artificial surfaces exclusion, whereas NGRDI helped for the differentiation of arboreal crops from low vegetation.
Arboreal false	VV-VH mean (2019-2020) < -15 PBS ≥ 30 (no vegetation)	In order to remove errors occurring in arboreal crops classification, PBS map and Sentinel-1 biannual composite were used.
Vineyards	$NDVI_{Apr} < NDVI_{May} < NDVI_{Jun}$ $NDVI_{Nov} < NDVI_{Oct}$ $NDVI_{Aug} < 0.50$ $NDVI_{max} < 0.80$ $NDVI_{min} > 0.10$ $\rho NIRNDVI_{max} > 4100$	Vineyard classification was based on vine phenological cycle, characterized by a growing season in spring and summer and a dormancy in autumn and winter. NDVI time series (Figure 6) was used for the recognition of these phenological stages. In addition, it was observed that the NIR reflectance of vineyards registered in the month in which the highest photosynthetic activity is recorded ($NDVI_{max}$), is always lower compered to arable lands, thus this characteristic was used for better discrimination between these two types of crops.
Irrigated arable lands	$NDVI_{max} > 0.50$ $4 < Time_{max} < 10$	Irrigated arable lands were classified on the basis of the assumption that i) Sardinian agricultural techniques involve a typical irrigation season between April and October, with a strong photosynthetic activity during this period (Figure 6), ii) an increasing trend during the first months of the season (May, April and July).
	$NDVI_{May} > 0.50$ $NDVI_{Jun} > 0.50$ $NDVI_{Jul} > 0.50$ $NDVI_{May} < NDVI_{Jun} < NDVI_{Jul}$	
Rice fields	$NDVI_{max} > 0.40$ $150 < Time_{max} < 250$ (DoY) $NDFI_{flood} > 0$ $Time_{flood} < Time_{max}$ $Probability_{flood} < 10\ \%$ $CP_{flood} < 80\ \%$ $Time_{flood}^1 \neq Time_{flood}^2$	Rice cultivation may involve the distinctive practice of flooding of the fields (usually during spring) before the establishment of the crop and successive rapid growth of rice plants, with the maximum photosynthetic activity reached in summer and the maturation in October, before the harvest. The detection of rice fields from satellite data is usually achieved through the recognition of the flooding signal (Boschetti et al., 2014). This signal can be identified by positive values of the NDFI index, registered before the growth of rice plants (Boschetti et al., 2017). For rice fields classification the detailed NDVI and NDFI time series were used to detect the flooding condition and phenological stages of rice (Figure 6). However, residual cloud contamination may cause positive values of NDFI. To reduce this issue, pixels presenting isolated positive values of NDFI, occurred with a cloud probability higher than 10% and a cloudy pixel percentage (CP) of the source image higher than 80% were excluded.
Non-irrigated arable lands	All the pixel not classified in previous steps	All the pixels not classified as irrigated arable land were automatically classified as non-irrigated arable lands, because they don't show a peak of photosynthetic activity from April to October, thus it was assumed that they are rainfed.

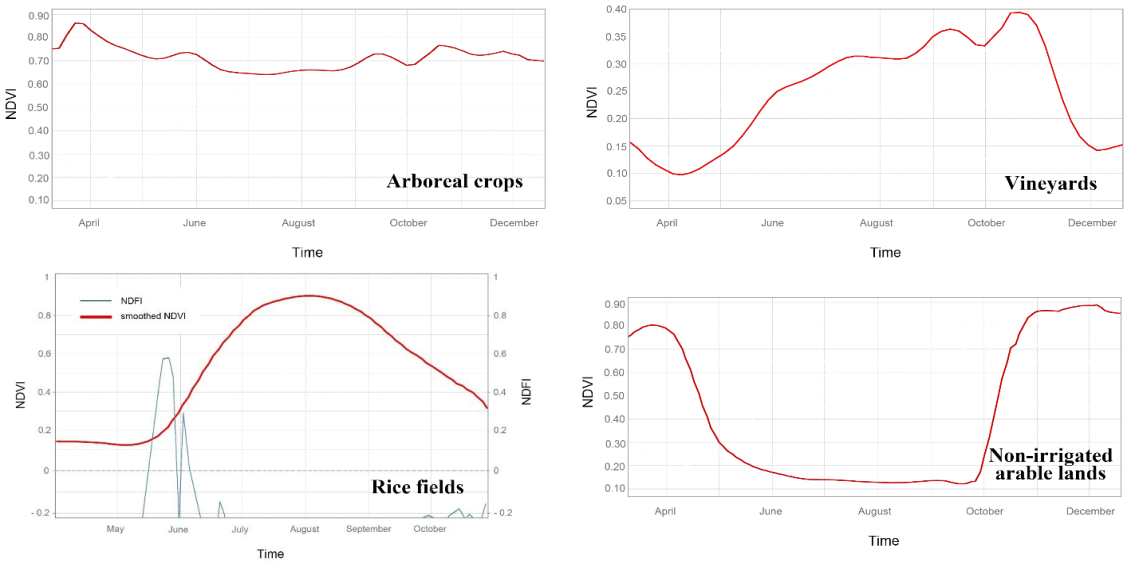

Figure 6. Examples of smoothed NDVI time series extracted from an arboreal crop (coniferous cultivation), a vineyard, a rice field and a non-irrigated arable land. While arboreal crops show a stable trend of NDVI during the year, vineyard and rice fields exhibit a marked peak of NDVI in August and November respectively, whereas non-irrigated lands don't present a photosynthetic activity during dry season (from May to October).

4.4 The Land cover map

Final land cover map resulting from the visual inspection process has a smaller number of polygons, compared to the preliminary map obtained from segmentation and pre-labelling of segments. Given the high fragmentation of the dataset introduced with the satellite image segmentation procedures, it is possible to note that, if, on the one hand this operation is particularly expensive in terms of time due to the high number of polygons, on the other the output product possesses undeniable characteristics of quality with richness and detail of information that are unusual and unattainable with traditional techniques.

4.5 Validation

In order to test the accuracy of the preliminary map derived from segmentation and pre-labelling, the same area selected for visual inspection was chosen for validation tests. A first validation analysis has been carried out through a ground truth data collected from a detailed photo-interpretation, by integrating data coming from different platforms and from several observations, as follows: digital orthophotos available for different years; Google Earth satellite images; Google Street View at street level images; Sentinel spectral index processing; Field observations; Previous knowledge of the locations by the authors. From the resulting map, polygons representing non-irrigated crops have been chosen to achieve validation as described below. A first set of 115 polygons has been selected with a minimum surface of 50,000 m2. The choice of this extent has been made to better take into consideration pixels with no contaminations by adjacent, different classes. For each polygon has been considered his centroid and a relative square buffer sized 9x9 pixels (8,100 m2). Due to geometric factors from the total amount only 67 square areas have been selected as training sites. This layer has been faced up to the classified product by an intersection overlay operation in order to verify the presence of land cover classes and their relative abundance. Crossing the datasets, we obtained 97% of correspondence for non-irrigated crops.

5. CONCLUSIONS

The land cover map realized in this study shows a high level of detail especially in complex landscapes such as green urban areas, rural fabrics as well as in small water bodies and trees outside forest, indicating an important improvement compared to existing land cover/use maps of Sardinia and demonstrating the potential of Sentinel imagery in the creation of thematic maps. Although not fully validated at regional scale, preliminary statistics show an extent of agricultural areas (non-irrigated arable, irrigated and greenhouses, 18,3%, 6,6% and 0,1 respectively, corresponding to 25% of the total area of Sardinia. Although this amount does not include agroforestry, arboreal and permanent crops accounting for an extra 8,5%, it is much higher compared to the 10% reported by ESA WorldCover map (Figure 2). This discrepancy can be narrowed down by removing greenhouses and pastures since they are considered by ESA as "Build-up" and "Grassland" respectively. Assessing the proportion of pasture and arable lands within the proposed map will be subject of further investigation. However, ISTAT (http://dati.istat.it/Index.aspx?DataSetCode=DCSP_COLTIVAZIONI) estimates that in 2020 pastures account for 68.1% of the total non-irrigated arable lands in the region, and thus, cutting out 5,7% from the abovementioned non-irrigated arable areas (18.3%), the final estimate can be reduced to 12,6%. This result is higher compared to the 11% reported by ISTATS in 2020, but not remarkably, considering the potential confusion between pastures and natural grassland, even in the existing thematic maps used as starting point in the classification. The results are encouraging even if some limitations have been found namely the confusion between natural tree cover and olive trees or fruit plants. The high variety of crop types and the different agricultural practices adopted by the farmers can negatively affect the accuracy of the automatic classification based on spectral and temporal indices thresholding. For these reasons, further studies are foreseen in order to overcome these issues.

ACKNOWLEDGEMENTS

This study has been supported by the Directorate General of the Regional Agency of the Hydrographic District of Sardinia in the framework of the "Activities of realization of the cartography of the Sardinian soil cover and of the monitoring system of the irrigated areas of Sardinia from remote sensing data".

REFERENCES

Afrasinei G.M., Melis M.T., Bradd, J.M., Buttau C., Arras C., Ghiglieri G., (2017). Assessment of remote sensing-based classification methods for change detection of salt-affected areas (Biskra area, Algeria). Journal of Applied Remote Sensing, vol. 11, p. 1-28, ISSN: 1931-3195, doi: 10.1117/1.JRS.11.016025

Afrasinei G.M., Melis M.T., Arras C., Pistis M., Buttau C., Ghiglieri G., 2018. Spatiotemporal and spectral analysis of sand encroachment dynamics in southern Tunisia. European Journal of Remote Sensing. Volume 51, 2018 - Issue 1. https://doi.org/10.1080/22797254.2018.1439343

Bansal S., Katyal D., and Garg J. K. (2017), "A novel strategy for wetland area extraction using multispectral MODIS data," Remote Sensing of Environment, vol. 200, pp. 183–205, doi: 10.1016/j.rse.2017.07.034.

Baatz M. and Schape A. (2000), "Multiresolution Segmentation - An Optimization Approach for High Quality Multi-Scale Image Segmentation.", Strobl, J., Blaschke, T. and Griesebner, G., Eds., Angewandte geographische informations verarbeitung, Heidelberg, 12-23.

Boschetti M., Busetto L., Manfron G., Laborte A., Asilo S., Pazhanivelan S., Nelson A. (2017), "PhenoRice: A method for automatic extraction of spatio-temporal information on rice crops using satellite data time series," Remote Sensing of Environment, vol. 194, pp. 347–365, doi: 10.1016/j.rse.2017.03.029.

Boschetti M., Nutini F., Manfron G., Brivio P. A., and Nelson A. (2014), "Comparative Analysis of Normalised Difference Spectral Indices Derived from MODIS for Detecting Surface Water in Flooded Rice Cropping Systems," PLoS ONE, vol. 9, no. 2, Art. no. 2, doi: 10.1371/journal.pone.0088741.

Castillo J. A. A., Apan A. A., Maraseni T. N., and Salmo S. G (2017), "Estimation and mapping of above-ground biomass of mangrove forests and their replacement land uses in the Philippines using Sentinel imagery," ISPRS Journal of Photogrammetry and Remote Sensing, vol. 134, pp. 70–85, doi: 10.1016/j.isprsjprs.2017.10.016.

D'Andrimont R., Verhegghen A., Lemoine G., Kempeneers P., Meroni M., van der Velde M. (2021), "From parcel to continental scale – A first European crop type map based on Sentinel-1 and LUCAS Copernicus in-situ observations", Remote Sensing of Environment, Volume 266, 112708, ISSN 0034-4257, doi: 10.1016/j.rse.2021.112708.

De Simone, L., Navarro, D., Gennari, P., Pekkarinen, A., de Lamo, J. (2021), "Using Standardized Time Series Land Cover Maps to Monitor the SDG Indicator "Mountain Green Cover Index" and Assess Its Sensitivity to Vegetation Dynamics", ISPRS Int. J. Geo-Inf., 10, 427, doi: 10.3390/ijgi10070427.

Faridatul M. I. and WuB. (2019), "Multi-Temporal Urban Land Cover Mapping Using Spectral Indices", doi: 10.5281/ZENODO.2580954.

Itzerott S., & Kaden K (2006), "Crop Classification Based on Spectral Standard Curves" 2nd Workshop of the EARSeL Special Interest Group on Land Use & Land Cover (Bonn 2006).

Eva H., Simonetti D., Marelli A., (2015). "IMPACT: portable GIS toolbox for image processing and land cover mapping", Publications Office. https://data.europa.eu/doi/10.2788/143497.

Mullissa A., Vollrath A., Odongo-Braun C., Slager B., Balling J., Gou Y., Gorelick N., Reiche J. (2021), "Sentinel-1 SAR Backscatter Analysis Ready Data Preparation in Google Earth Engine," Remote Sensing, vol. 13, no. 10, Art. no. 10, doi: 10.3390/rs13101954.

Pageot Y., Baup F., Inglada J., Baghdadi N., and Demarez V. (2020), "Detection of Irrigated and Rainfed Crops in Temperate Areas Using Sentinel-1 and Sentinel-2 Time Series," Remote Sensing, vol. 12, no. 18, Art. no. 18, Sep., doi: 10.3390/rs12183044.

Qian Y., Zhou W., Nytch C. J., Han L., and Li Z. (2020), "A new index to differentiate tree and grass based on high resolution image and object-based methods," Urban Forestry & Urban Greening, vol. 53, p. 126661, doi: 10.1016/j.ufug.2020.126661.

Qu C. and Li P. (2020), "Winter Wheat Mapping from Landsat NDVI Time Series Data Using Time-Weighted Dynamic Time Warping and Phenological Rules,", doi: 10.1109/igarss39084.2020.9323243.

Simonetti D., Pimple U., Langner A., and MarelliA. (2021), "Pan-tropical Sentinel-2 cloud-free annual composite datasets," Data in Brief, vol. 39, p. 107488, doi: 10.1016/j.dib.2021.107488.

Simonetti D., Simonetti E., Szantoi Z., Lupi A., and Eva H. D. (2015), "First Results From the Phenology-Based Synthesis Classifier Using Landsat 8 Imagery," IEEE Geoscience and Remote Sensing Letters, vol. 12, no. 7, Art. no. 7, doi: 10.1109/lgrs.2015.2409982.

Sinha P., Virma N.K., Atumo E.A. (2016) "Urban Built-up Area Extraction and Change Detection of Adama Municipal Area using Time-Series Landsat Images," International Journal of Advanced Remote Sensing and GIS, vol. 5, no. 1, Art. no. 1, doi: 10.23953/cloud.ijarsg.67.

Sonobe R., Sano T., and Horie H. (2018), "Using spectral reflectance to estimate leaf chlorophyll content of tea with shading treatments," Biosystems Engineering, vol. 175, pp. 168–182, doi: 10.1016/j.biosystemseng.2018.09.018.

Wang Z., Liu J., Li J., and Zhang D. (2018), "Multi-Spectral Water Index (MuWI): A Native 10-m Multi-Spectral Water Index for Accurate Water Mapping on Sentinel-2," Remote Sensing, vol. 10, no. 10, Art. no. 10, doi: 10.3390/rs10101643.

Zanaga, D., Van De Kerchove, R., De Keersmaecker, W., Souverijns, N., Brockmann, C., Quast, R., Wevers, J., Grosu, A., Paccini, A., Vergnaud, S., Cartus, O., Santoro, M., Fritz, S., Georgieva, I., Lesiv, M., Carter, S., Herold, M., Li, Linlin, Tsendbazar, N.E., Ramoino, F., Arino, O. (2021), "ESA WorldCover 10 m 2020 v100", doi: 10.5281/ZENODO.5571936.